INTERNATIONAL JOURNAL OF ROBOTICS
(THEORY AND APPLICATIONS)
E-mail: IJR@kntu.ac.ir

Modeling and Optimal Control of 4 Wheel Steering Vehicle Using LQR and its Comparison with 2 Wheel Steering Vehicle

H. Tourajizadeh [a], M. Sarvari[b] and A. S. Ordoo[c,]

[a] Assistant prof., Mechanical Engineering Department, Faculty of Engineering, Kharazmi University, Tehran, Iran

[b] MSc. Student., Mechanical Engineering Department, Faculty of Engineering, Kharazmi University, Tehran, Iran

[c] MSc., Mechanical Engineering Department, Faculty of Engineering, Kharazmi University, Tehran, Iran

ARTICLE INFO

Article history:

Received: 7 June 2019

Received in revised form: 21 January 2020

Accepted: 1 February 2020

Keywords:

4 Wheel Steering Vehicle

Optimal Control

Jacobian Based Kinematics

LQR

ABSTRACT

In this paper, kinetic and kinematic modeling of a 4 wheel steering vehicle is done and its movement is controlled in an optimal way using Linear Quadratic Regulator (LQR). The results are compared with the same control of two-wheel steering case and the advantages are analyzed. In 4 wheel steering vehicles which are nowadays more applicable the number of controlling actuators are more than the required actuators for controllability of the system. As a result, the possible path through which he vehicle can move to transfer between two boundaries is not unique and this fact provides the possibility of optimization of a desired cost function. In this paper after extracting the model of these vehicles based on Jacobian matrix a compromise between the accuracy and controlling effort is selected as the mentioned objective function and the optimal control and its related optimal path is extracted through which the best accuracy and the least input is required. The correctness of modeling and efficiency of the designed optimal controller is verified by the aid of a series of simulation scenarios and also comparing the results between 4 wheel steering vehicles and 2 wheel steering ones.

1. Introduction

4 wheel steering vehicles are the new generation of vehicle in which not only the front wheels are steerable but also the rear ones can be steered too. This modification increases the number of controlling input while the number of workspace states are constant. This fact increases the maneuverability of the vehicle and provides the possibility of optimization or constraint satisfaction during transferring the vehicle between two definite boundaries. The constraint satisfaction or optimization can be subject to different cost functions. The most important application of this kind of optimization is parallel parking in which the required distance for realizing the displacement between two challenging boundaries is significantly less for the mentioned 4wheel steering vehicle compared to 2 wheel steering one. One of the first issues addressed in the study of 4WS is the analysis of kinematics and dynamic model, who Spentzas with a particular view made a comparison and provided various states of 2WS and 4WS. He studied another form of the model through exploring bicycle model in 4WS state.[1, 2] Singh also analyzed and compared 4WS and 2WS and provided the pros and cons of them. Furthermore, he provided importance and functional states for 4WS [3]. But, in these states, there is no analysis of control. Wang developed a path planning algorithm base on 4WS vehicle kinematics in which velocity and steering angle

are two main parts in this algorithm.[4] By exploring and experimenting on 4WS and 4WD tractors on smooth road, Itoh addressed the effect of velocity on body yaw rate and side slip angle which is possible by providing dynamic model.[5].In these cases, there is no analysis of optimal control inputs. Also, kinematic and kinetic analyses have been conducted in various models of robot.[6] Xao studied controllability and stability of non-holonomic robot through forward and inverse kinematics and dynamics. But, no control input have not been defined and optimized. In most of the functional control algorithms of 4WS used by Haiyan, there is a relative gain defined between front and rear wheels steering angles. But, this method has only one independent control input and process of optimization is impossible.[7] Taheri through applying Lyapanov stability theory on 4WS model and considering control strategy and adaptability rules obtained yaw rate and desired lateral velocity.[8] The optimization algorithms of these kind of robots can be divided into two main categories of open loop and closed loop optimization. In open loop optimization, the optimal path of the system is extracted subject to the constraints of dynamic equations of the vehicle using variation calculations. However, these kind of optimizations are not robust against uncertainties or external disturbances while the feedback of the states are not engaged in. The closed loop optimization on the other hand provides a robust optimization process which itself can be divided again to linear and nonlinear optimization. Linear optimizations like Linear Quadratic Regulator (LQR) are mostly suitable for the plants with linear dynamics while nonlinear ones can provide optimization of nonlinear system with higher range of workspace. Korayem provided an online computational algorithm for tricycle wheeled robots which provides and optimal and smooth trajectory with external obstacles for actuators, in a way that it reaches the desired final point with optimal inputs and without encounter with obstacles. A non-holonomic constraint is applied on the dynamics of this robot type and a matrix has been defined for connection between joint space and work space. For 4WS, such connection has not been defined yet.[9] In [10] one vehicle is adaptively controlled in a way that there is one wheel for control input. Adaptive control strategy used in this article is based on low level and high level method. but, here optimization of control input is overlooked and only the front wheels change their orientations. One of the most important advantage of 4WS vehicle is their high capability for optimization in time of increased number of inputs while the number of freedom degree is constant. Higuchi suggested an optimal control strategy for 4WS which is based on linear quadratic regulation (LQR).[11] Also, similar optimal control strategy in [12] is used by Siahkalroudi in which there are compensators ZSS and ZYR for the linearized model. Furthermore, Mostavi used a pole replacement method for stability of linearized system while it was controlled by linear quadratic regulation (LQR).[13] In the mentioned cases, no comparison was made between control input values of 4WS and 2WS. Suggesting an integrator control system, Yuqing provided a proper performance for non-linear behavior of vehicle's wheels and obtained optimal steering angle for front and rear wheels.[14] In [15], providing 4WS dynamic model and considering only the angles of front and rear wheels as control input, Hongming analyzed optimal adaptive control. The amount of wheel force is not mentioned in previous articles, but in the present article is considered. Akita in [16] studied 4WS vehicle and controlled rear steering of wheel using H_∞ method which is considered as an adaptive control method. This case considers instability of trailer. But, rear steering angle control is not enough alone and non-linear model converted to linear model. Lee helped stability of vehicle moving in a direct path encountering lateral wind by stability and steering booster systems and combining low level controllers using parametric optimization method.[17] Suggested control method in this article has more validity in comparison to parametric optimization method. Meanwhile, in the mentioned case, the optimization related to applied force on wheels has not been analyzed. For determining status of two lateral and orientation motion state variables, Matsumoto, in addition to front steering angle, considered a control input and compared the results of linear quadratic regulation method (LQR) to experimental method.[18] It can be seen that in the previous researches the velocity kinematics of the vehicle is not extracted by the aid of Jacobian matrix of the vehicle which is a perquisite of controlling of the system. Also the optimization process is not compared between 2 wheel steering vehicles and 4 wheel steering ones to illustrate the efficiency of the optimization process for the latter cases. To cover the mentioned goals, in this paper first of all a bicycle model of 4 wheel steering vehicle is considered to extract the kinematic model of the system using Jacobian matrix. Afterwards the dynamics of the same model is modeled considering the dynamics and sliding effect of the tires using Newton-Euler method. Afterwards both of 2 wheel steering vehicles and 4 wheel steering ones are controlled in an optimal way using LQR to extract the optimal path between two definite boundaries and compare the results for these two kind of plants. The reason of applicability of linear optimization tool of LQR for nonlinear dynamics of vehicle is contributed to this fact that the linearization of vehicle state space around an operating point can be considered satisfactorily valid for small and even average range of vehicle movement between two boundaries like parallel parking. In order to check the correctness of modelling, robustness of the controller and also efficiency of the optimization, some analytic and comparative simulation scenarios are performed in MATLAB and the superiority of 4 wheel steering case is proved during the optimization process over 2 wheel steering ones. Finally it is shown that the proposed optimization method for the proposed model of vehicle can successfully guide

the vehicle between two definite boundaries with the best accuracy and least amount of energy consumption.

2. Kinematic and Kinetics Modeling

2.1. Kinematics Model

There are two methods for modeling vehicle; one methods is to consider both the front wheel and rear wheel as the two wheels. This method in known as two wheel model. The second method is to revealing the equations between all four wheels and there is no simplification. Thus, we face more nonlinearity. As mentioned before, in this paper we use the first model i.e. bicycle model, for control analysis. In figure 1, the bicycle model is shown as schematic in which the front and rear wheels are rotating, each having different angle. There are some assumptions for kinematic modeling through which we can attain a more simplified model. For analyzing kinematics of vehicle according to figure 1, we assume there is palatal rigid body motion and no wheel slip exists for bicycle model in X-Y fixed coordinate plane. With regard to figure 1, point C is considered as the center of gravity and the coordinate of this point represents the location of vehicle on fixed coordinate system. Vector V is linear velocity of vehicle in the center of gravity which in fact is the angle between longitudinal axis of vehicle and X coordinate. Ψ is the heading angle of vehicle. Side-slip angle β is the angle between linear velocity vector of center of gravity and longitudinal axis of vehicle. v_f and v_r are linear velocity of front and rear wheels in virtual location of wheels in bicycle model, respectively. δ_f and δ_r are steering angle of front and rear wheels, respectively; that is the angles between longitudinal axis of each wheel and longitudinal axis of vehicle. lf is defined as the distance from the center of gravity of vehicle to axis of front wheel and l_r is defined as the distance from the center of gravity of vehicle to axis of rear wheel. According to figure 1, kinematics equations is as follows: [4]

$$\dot{X} = V\cos(\psi+\beta) \tag{1}$$

$$\dot{Y} = V\sin(\psi+\beta) \tag{2}$$

$$\dot{\psi} = \frac{V\cos\beta(\tan\delta_f - \tan\delta_r)}{l_f + l_r} \tag{3}$$

$$\beta = \tan^{-1}\left(\frac{l_r\tan\delta_f + l_f\tan\delta_r)}{l_f + l_r}\right) \tag{4}$$

$$V = \frac{v_f\cos\delta_f + v_r\cos\delta_r)}{2\cos\beta} \tag{5}$$

In equation 5, if we define linear velocity of each wheel according to the angular velocity of that wheel, we have:

$$V = \frac{(r\omega_f)\cos\delta_f + (r\omega_r)\cos\delta_r)}{2\cos\beta} \tag{6}$$

In which, r represents radius of each wheel. In this model, by considering angular velocities of wheels (ω_f,ω_r) as input and their relations with state variables ($\dot{X}$, $\dot{Y}$,$\dot{\psi}$), it can be possible to define certain matrices which contain general rotation of vehicle and velocity of each wheel.

$$\begin{Bmatrix}\dot{X}\\ \dot{Y}\\ \dot{\psi}\end{Bmatrix} = J_a\begin{Bmatrix}\omega_f\\ \omega_r\end{Bmatrix} \tag{7}$$

$$[J_a] = [R][J] \tag{8}$$

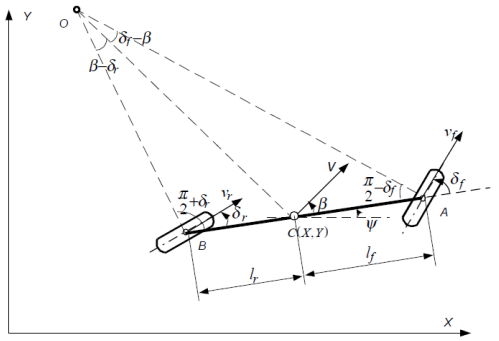

Figure 1. Bicycle model of the vehicle for kinematic modeling.

$$[J_a] = \begin{bmatrix}\cos\psi & -\sin\psi & 0\\ \sin\psi & \cos\psi & 0\\ 0 & 0 & 1\end{bmatrix}\times\begin{bmatrix}\frac{r}{2}\cos\delta_f & \frac{r}{2}\cos\delta_r\\ \frac{r}{2}\cos\delta_f\tan\beta & \frac{r}{2}\cos\delta_r\tan\beta\\ \frac{r}{2l}\cos\delta_f(\tan\delta_f-\tan\delta_r) & \frac{r}{2l}\cos\delta_r(\tan\delta_f-\tan\delta_r)\end{bmatrix} \tag{9}$$

In equation (9), $l_f + l_r$ equals l which is defined as the distance of rear and front axis. By substituting beta value from equation (4) to equation (9), we can obtain matrix J_a according to steering wheel angle and general rotation of vehicle.

$$[J_a] = \begin{bmatrix}J_{a11} & J_{a12}\\ J_{a21} & J_{a22}\\ \frac{r(\tan\delta_f-\tan\delta_r)}{2l}\cos\delta_f & \frac{r(\tan\delta_f-\tan\delta_r)}{2l}\cos\delta_r\end{bmatrix} \tag{10}$$

$$J_{a11} = \frac{r}{2}\left(\cos\psi - \sin\psi\left(\frac{l_r\tan\delta_f + l_f\tan\delta_r)}{l}\right)\right)\cos\delta_f$$

$$J_{a12} = \frac{r}{2}\left(\cos\psi - \sin\psi\left(\frac{l_r\tan\delta_f + l_f\tan\delta_r)}{l}\right)\right)\cos\delta_r$$

$$J_{a21} = \frac{r}{2}\left(\sin\psi + \cos\psi\left(\frac{l_r\tan\delta_f + l_f\tan\delta_r)}{l}\right)\right)\cos\delta_f$$

$$J_{a22} = \frac{r}{2}\left(\sin\psi + \cos\psi\left(\frac{l_r\tan\delta_f + l_f\tan\delta_r)}{l}\right)\right)\cos\delta_r$$

It can be seen that in equation (7), by having steering wheel angle velocity as their joint spaces and steering angles, we can obtain work space parameters. It should be mentioned that for having $\dot{\psi}$ on the right side of equation, we must with the third joint space , in simulation software using integrator and defining initial

values. Further, it is possible to obtain joint space from work space in inverse state. This allows us to have a proper verification for extracted equations. The results obtained from forward and inverse kinematics are shown in following pages.

2.2. Kinetic model

As mentioned before, the bicycle model is a known model for vehicle modeling in which the front and rear wheels are considered as two wheels. In this article, this model is used for dynamic analysis. Dynamic of bicycle model is shown in figure 2. In this figure, the front and rear wheels have different angles. Longitudinal and lateral friction forces applied on wheels are F_{li} and F_{si} respectively. If we write dynamic equations for vehicle, then we obtain state space equations for the system. In fact, dynamic equations for system is of significant importance because it spans all the necessary state space for applying different controls. In the present article, Newton-Euler method has been used for obtaining dynamic equations for the system. With the assumption of fixed coordinate of inertia system and coordinate of center of gravity, the velocity equations are expressed according to (11):

$$\begin{bmatrix} \dot{X} \\ \dot{Y} \end{bmatrix} = V \begin{bmatrix} \cos(\beta+\psi) \\ \sin(\beta+\psi) \end{bmatrix} \tag{11}$$

After derivative:

$$\begin{bmatrix} \ddot{X} \\ \ddot{Y} \end{bmatrix} = V\left(\dot{\beta}+\dot{\psi}\right)\begin{bmatrix} -\sin(\beta+\psi) \\ \cos(\beta+\psi) \end{bmatrix} + \dot{V}\begin{bmatrix} \cos(\beta+\psi) \\ \sin(\beta+\psi) \end{bmatrix} \tag{12}$$

And transporting of fixed coordinate of inertia to coordinate of center of gravity:

$$\begin{bmatrix} \ddot{x} \\ \ddot{y} \end{bmatrix} = \begin{bmatrix} \cos\psi & \sin\psi \\ -\sin\psi & \cos\psi \end{bmatrix}\begin{bmatrix} \ddot{X} \\ \ddot{Y} \end{bmatrix} = V\left(\dot{\beta}+\dot{\psi}\right)\begin{bmatrix} -\sin\beta \\ \cos\beta \end{bmatrix} + \dot{V}\begin{bmatrix} \cos\beta \\ \sin\beta \end{bmatrix} \tag{13}$$

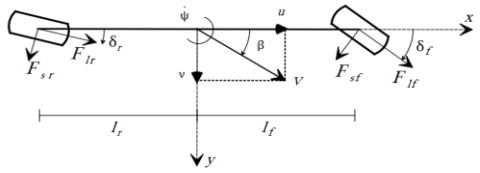

Figure 2. Bicycle model of the vehicle for dynamic modeling.

With the assumption of lack of gravity forces, rolling resistance and velocity and wind force, the equation of vehicle's longitudinal motion using Newton's second law is as (14):

$$V\left(\dot{\beta}+\dot{\psi}\right)\begin{bmatrix} -\sin\beta \\ \cos\beta \end{bmatrix} + \dot{V}\begin{bmatrix} \cos\beta \\ \sin\beta \end{bmatrix} = \frac{1}{M}\begin{bmatrix} F_{xf}+F_{xr} \\ F_{yf}+F_{yr} \end{bmatrix} \tag{14}$$

Here, M is the mass of vehicle. If two rows of matrix equation of (14) divides into two algebraic equation:

$$-V\left(\dot{\beta}+\dot{\psi}\right)\sin\beta + \dot{V}\cos\beta = \frac{1}{M}\left(F_{xf}+F_{xr}\right) \tag{15}$$

$$V\left(\dot{\beta}+\dot{\psi}\right)\cos\beta + \dot{V}\sin\beta = \frac{1}{M}\left(F_{yf}+F_{yr}\right) \tag{16}$$

If equation (15) is the product of cosβ and equation of (16) is the product of sinβ:

$$\begin{aligned} -V\left(\dot{\beta}+\dot{\psi}\right)\sin\beta\cos\beta + \dot{V}\cos^2\beta &= \frac{\cos\beta}{M}\left(F_{xf}+F_{xr}\right) \\ V\left(\dot{\beta}+\dot{\psi}\right)\cos\beta\sin\beta + \dot{V}\sin^2\beta &= \frac{\sin\beta}{M}\left(F_{yf}+F_{yr}\right) \end{aligned} \tag{17}$$

By summing two equations of (17), we obtain the equation of velocity derivate:

$$\dot{V} = \frac{\cos\beta}{M}\left(F_{xf}+F_{xr}\right) + \frac{\sin\beta}{M}\left(F_{yf}+F_{yr}\right) \tag{18}$$

From equation (16) we can obtain equation based on slide slip angle:

$$\dot{\beta} = \frac{1}{MV\cos\beta}\left(F_{yf}+F_{yr}-M\dot{V}\sin\beta\right) - \dot{\psi} \tag{19}$$

With regard to Euler equation for dynamic model, we will have:

$$J\ddot{\psi} = F_{yf}.(l_f - n_f) - F_{yr}.(l_r + n_r) \tag{20}$$

n_f is the distance of contact point of front wheel with ground to lateral axis front chassis and n_r is the distance of contact point of rear wheel with ground to lateral axis rear chassis. And J is mass moment of Inertia. By replacing:

$$\begin{aligned} F_{xi} &= F_{li}\cos\delta_i - F_{si}\sin\delta_i \\ F_{yi} &= F_{si}\cos\delta_i + F_{li}\sin\delta_i \end{aligned} \tag{21}$$

In which notation i includes r and f, representing front and rear axis of vehicle. further, lateral force applied on each wheel is in relation with side slip angles.

$$\begin{aligned} F_{sf} &= C_f.\alpha_f = C_f(\delta_f - \beta - \frac{l_f.\dot{\psi}}{V}) \\ F_{sr} &= C_r.\alpha_r = C_r(\delta_r - \beta + \frac{l_r.\dot{\psi}}{V}) \end{aligned} \tag{22}$$

C_f is cornering stiffness of front wheel and C_r is cornering stiffness of rear wheel. Furthermore, α_f is side slip angle for front wheel and α_r is slide slip angle for rear wheel. Therefore, equations (18-20) convert to equations (20-25).

$$f_1 = \dot{V} = \frac{1}{M}\{F_{lf}\cos(\beta-\delta_f)+F_{lr}\cos(\beta-\delta_r) + C_f\left[\delta_f-\beta-\frac{l_f\dot{\psi}}{V}\right]\sin(\beta-\delta_f)+C_r\left[\delta_r-\beta+\frac{l_r\dot{\psi}}{V}\right]\sin(\beta-\delta_r)\} \quad (23)$$

$$f_2 = \dot{\beta} = \frac{1}{MV}\{-F_{lf}\sin(\beta-\delta_f)-F_{lr}\sin(\beta-\delta_r)+ C_f\left[\delta_f-\beta-\frac{l_f\dot{\psi}}{V}\right]\cos(\beta-\delta_f)+C_r\left[\delta_r-\beta+\frac{l_r\dot{\psi}}{V}\right]\cos(\beta-\delta_r)\}-\dot{\psi} \quad (24)$$

$$f_3 = \ddot{\psi} = \frac{1}{JV}\{F_{lf}Vl_f\sin(\delta_f)+C_f\left[\delta_f l_f V-\beta l_f V-l_f^2\dot{\psi}\right]\cos(\delta_f) -F_{lr}Vl_r\sin(\delta_r)+C_r\left[-\delta_r l_r V+\beta l_r V-l_r^2\dot{\psi}\right]\cos(\delta_r) -V\left[F_{lf}n_f\sin(\delta_f)+F_{lr}n_r\sin(\delta_r)\right]+n_f C_f\left[(\beta-\delta_f)V+l_f\dot{\psi}\right]\cos(\delta_f) +n_r C_r\left[(\beta-\delta_r)V-l_r\dot{\psi}\right]\cos(\delta_r)\} \quad (25)$$

It can be seen that 3 state variables exist in equations (23-25).

3. Optimal control of 4WS vehicle using LQR method

Linear quadratic regulator is one of the optimal control methods which regulates system control input and its states, with regard to constraints on dynamic system, for obtaining optimal output. Equations (23-25) is rewritten in the form of state space according to equation (26).

$$\dot{x} = A(x,u)x + B(x,u)u \quad (26)$$

Which vector x is state variables vector and is defined according to equation (27).

$$\underline{x} = \begin{Bmatrix} V \\ \beta \\ \dot{\psi} \end{Bmatrix} \quad (27)$$

And vector u is the control inputs for system which is defined according to equation (28).

$$\underline{u} = \begin{Bmatrix} F_{lf} \\ F_{lr} \\ \delta_f \\ \delta_r \end{Bmatrix} \quad (28)$$

State space equation obtained from non-linear dynamic equation for system are non-linear equations which should be optimized. Hence, state variables should be expressed according to Tylor series surrounding work space so that Jacobian matrices insert as multiplier matrices. In this way, state space equations can be linearized. Equations (29) and (30) express linearized multiplier matrices surrounding work space. Each of its entries are obtained using Jacobian of dynamic equation. [19]

$$A = \frac{\partial \underline{f}(\underline{x},\underline{u})}{\partial \underline{x}} = \begin{bmatrix} \frac{\partial f_1}{\partial x_1} & \frac{\partial f_1}{\partial x_2} & \frac{\partial f_1}{\partial x_3} \\ \frac{\partial f_2}{\partial x_1} & \frac{\partial f_2}{\partial x_2} & \frac{\partial f_2}{\partial x_3} \\ \frac{\partial f_3}{\partial x_1} & \frac{\partial f_3}{\partial x_2} & \frac{\partial f_3}{\partial x_3} \end{bmatrix} \quad (29)$$

$$\frac{\partial f_1}{\partial x_1} = \frac{\dot{\psi}}{MV^2}\left[C_f l_f\sin(\beta-\delta_f)-C_r l_r\sin(\beta-\delta_r)\right]$$

$$\frac{\partial f_1}{\partial x_2} = -\frac{1}{M}\{C_f\sin(\beta-\delta_f)+C_r\sin(\beta-\delta_r) +F_{lf}\sin(\beta-\delta_f)+F_{lr}\sin(\beta-\delta_r) +C_f\left(\beta-\delta_f+\frac{\dot{\psi}l_f}{V}\right)\cos(\beta-\delta_f) -C_r\left(-\beta+\delta_r+\frac{\dot{\psi}l_r}{V}\right)\cos(\beta-\delta_r)\}$$

$$\frac{\partial f_1}{\partial x_3} = -\frac{1}{MV}\left[C_f l_f\sin(\beta-\delta_f)-C_r l_r\sin(\beta-\delta_r)\right]$$

$$\frac{\partial f_2}{\partial x_1} = \frac{1}{MV^2}\{F_{lf}\sin(\beta-\delta_f)+F_{lr}\sin(\beta-\delta_r) +C_f\left[-\delta_f+\beta+\frac{l_f\dot{\psi}}{V}\right]\cos(\beta-\delta_f) -C_r\left[\delta_r-\beta+\frac{l_r\dot{\psi}}{V}\right]\cos(\beta-\delta_r)\} +\frac{\dot{\psi}}{MV^3}\left[C_f l_f\cos(\beta-\delta_f)-C_r l_r\cos(\beta-\delta_r)\right]$$

$$\frac{\partial f_2}{\partial x_2} = -\frac{1}{MV}\{C_f\cos(\beta-\delta_f)+C_r\cos(\beta-\delta_r)+F_{lf}\cos(\beta-\delta_f) +F_{lr}\cos(\beta-\delta_r)-C_f\left[-\delta_f+\beta+\frac{l_f\dot{\psi}}{V}\right]\sin(\beta-\delta_f) +C_r\left[\delta_r-\beta+\frac{l_r\dot{\psi}}{V}\right]\sin(\beta-\delta_r)\}$$

$$\frac{\partial f_2}{\partial x_3} = -\frac{1}{MV^2}\left[C_f l_f\cos(\beta-\delta_f)-C_r l_r\cos(\beta-\delta_r)\right]-1$$

$$\frac{\partial f_3}{\partial x_1} = \frac{\dot{\psi}}{JV^2}\left[C_f l_f(l_f-n_f)\cos(\delta_f)+C_r l_r(l_r+n_r)\cos(\delta_r)\right]$$

$$\frac{\partial f_3}{\partial x_2} = \frac{1}{J}\left[C_f(n_f-l_f)\cos(\delta_f)+C_r(l_r+n_r)\cos(\delta_r)\right]$$

$$\frac{\partial f_3}{\partial x_3} = -\frac{1}{JV}\left\{C_f l_f(l_f-n_f)\cos(\delta_f)+C_r l_r(l_r+n_r)\cos(\delta_r)\right\}$$

(30)

$$B = \frac{\partial \underline{f}(\underline{x},\underline{u})}{\partial \underline{u}} = \begin{bmatrix} \frac{\partial f_1}{\partial u_1} & \frac{\partial f_1}{\partial u_2} & \frac{\partial f_1}{\partial u_3} & \frac{\partial f_1}{\partial u_4} \\ \frac{\partial f_2}{\partial u_1} & \frac{\partial f_2}{\partial u_2} & \frac{\partial f_2}{\partial u_3} & \frac{\partial f_2}{\partial u_4} \\ \frac{\partial f_3}{\partial u_1} & \frac{\partial f_3}{\partial u_2} & \frac{\partial f_3}{\partial u_3} & \frac{\partial f_3}{\partial u_4} \end{bmatrix}$$

$$\frac{\partial f_1}{\partial u_1} = \frac{\cos(\beta-\delta_f)}{M}$$

$$\frac{\partial f_1}{\partial u_2} = \frac{\cos(\beta-\delta_r)}{M}$$

$$\frac{\partial f_1}{\partial u_3} = \frac{1}{M}\left[(C_f+F_{lf})\sin(\beta-\delta_f)+C_f\left(\beta-\delta_f+\frac{\dot{\psi}l_f}{V}\right)\cos(\beta-\delta_f)\right]$$

$$\frac{\partial f_1}{\partial u_4} = \frac{1}{M}\left[(C_r+F_{lr})\sin(\beta-\delta_r)-C_r\left(-\beta+\delta_r+\frac{\dot{\psi}l_r}{V}\right)\cos(\beta-\delta_r)\right]$$

$$\frac{\partial f_2}{\partial u_1} = -\frac{\sin(\beta-\delta_f)}{MV}$$

$$\frac{\partial f_2}{\partial u_2} = -\frac{\sin(\beta-\delta_r)}{MV}$$

$$\frac{\partial f_2}{\partial u_3} = \frac{1}{MV}\left[(C_f+F_{lf})\cos(\beta-\delta_f)-C_f\left(\beta-\delta_f+\frac{\dot{\psi}l_f}{V}\right)\sin(\beta-\delta_f)\right]$$

$$\frac{\partial f_2}{\partial u_4} = \frac{1}{MV}\left[(C_r+F_{lr})\cos(\beta-\delta_r)+C_r\left(\delta_r-\beta+\frac{\dot{\psi}l_r}{V}\right)\sin(\beta-\delta_r)\right]$$

$$\frac{\partial f_3}{\partial u_1} = \frac{(l_f - n_f)\sin(\delta_f)}{J}$$

$$\frac{\partial f_3}{\partial u_2} = -\frac{(l_r + n_r)\sin(\delta_r)}{J}$$

$$\frac{\partial f_3}{\partial u_3} = \frac{(l_f - n_f)}{J}\left[(C_f + F_{lf})\cos(\delta_f) + C_f\left(\beta - \delta_f + \frac{\dot{\psi} l_f}{V}\right)\sin(\delta_f)\right]$$

$$\frac{\partial f_3}{\partial u_4} = -\frac{(l_r + n_r)}{J}\left[(C_r + F_{lr})\cos(\delta_r) - C_r\left(-\beta + \delta_r + \frac{\dot{\psi} l_r}{V}\right)\sin(\delta_r)\right]$$

In this method, considering the equation (21), state space equations for closed loop control system are obtained as equation (32).

$$u = -Kx \tag{31}$$

$$\dot{x} = Ax + Bu = (A - BK)x \tag{32}$$

Matrix K in equation (31) is the gain control matrix. The main objective of optimal control is to determine control signal of a system, which satisfy some of the physical constraints in a specific time, which by choosing a performance index reaches its desired minimum or maximum state. Optimal closed loop control is done using equations (31) and (32). With this difference, now K is optimal gain control obtained from minimizing cost function shown in equation (33).

$$J = \int (x^T Q x + u^T R u) dt \tag{33}$$

Matrices Q and R represent weight matrices of states space and system inputs, respectively, which determine the amount of sensitivity and significance of each of them. Therefore, for obtaining matrix K, We need to define weight matrices Q and R, depending on input significance and maximum error of output. There are many methods for determining these matrices.[20] The matrices can be chosen as R=1/max||u||and Q=1/max||x||. In which max ||x|| and max||u|| represent maximum error permitted tracking and maximum size of input control, respectively. In this article, considering system state, maximum size of input control for one of the inputs and maximum error permitted tracking for one of the state space are chosen max||x||=0.01 and max||u||=200 , respectively.at last, weight matrices entries are obtained according to equation (34).

$$Q = 100\begin{bmatrix} 90 & 0 & 0 \\ 0 & 100 & 0 \\ 0 & 0 & 1 \end{bmatrix},\ R = \begin{bmatrix} 5\times10^{-3} & 0 & 0 & 0 \\ 0 & 5\times10^{-3} & 0 & 0 \\ 0 & 0 & 10^{7} & 0 \\ 0 & 0 & 0 & 10^{7} \end{bmatrix} \tag{34}$$

Using equation (33) and (34) optimal gain control matrices are obtained using equation (35).

$$K = R^{-1}B^T S \tag{35}$$

In which, matric S is obtained through solving Riccati Equation (36). [21]

$$-A^T S - SA + SBR^{-1}B^T S - Q = 0 \tag{36}$$

4. Simulation

4.1. Kinematic simulation

For checking on verification of the equations for four wheel steering vehicle in bicycle model with the specifications provided in table 1, kinematic simulation are implemented and this verification is confirmed through comparison of the results of forward and inverse kinematics. In forward kinematics, we specify desired trajectory for angular velocity of wheels as the input and work space data is as output. In inverse kinematics, work space data is as input and angular velocity of wheels as output. In this article, comparison of the mentioned methods are verification of kinematics. Then, we compare angular velocities. Input trajectory function are defined according to equation (37).

$$\omega_f = 2t + 1$$
$$\omega_r = 1.8t + 4 \tag{37}$$

Table 1.Characteristics Of Simulated 4WS Vehicle

Name of the parameter	Sym	value	unit
Linear velocity at the mass center of the vehicle	V	25	m/s
Vehicle body sideslip	β	0.1047	rad
Vehicle body yaw angle rate	ψ	0.15	rad/s
Front steering angle	δf	0.4363	rad
Rear steering angle	δr	0.1747	rad
Vehicle mass	M	1600	kg
Mass moment of Inertia	J	2300	kg.m2
Distance from CoG to front axle	lf	1.2	m
Distance from CoG to rear axle	lr	1	m
Front tire longitudinal casters	nf	0.05	m
Rear tire longitudinal casters	nr	0.05	m
Cornering stiffness of front tire	Cf	29000	N/rad
Cornering stiffness of rear tire	Cr	60000	N/rad
Wheels radius	r	0.3	m

Accordingly, a comparison of forward and inverse kinematic angular velocities is obtained as shown in Figure 3. As it can been seen, there is an acceptable overlap between angular velocity of joint space for wheels in forward and inverse kinematics. Furthermore, there is a minimal error more pertinent to numerical

solve of non-linear kinematic equation using the software (MATLAB). Therefore, it can be concluded that the obtained result is verified. Also, work space fits with this joint space according to figure 4.

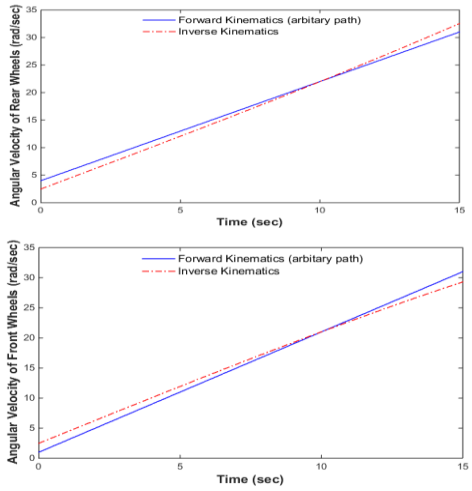

Figure 3.Comparison of the angular velocities of forward and inverse

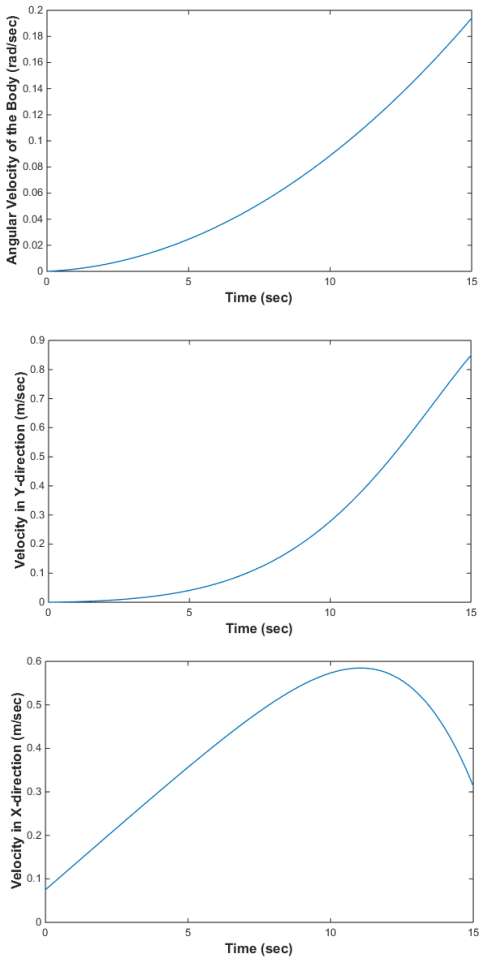

Figure 4. Workspace variables in kinematic simulation

4.2. Kinetic simulation

In order to validate the kinetic modeling, the same procedure which had been employed for kinematic section is performed. Kinetic specifications of 4WS has been provided earlier in table 1. Therefore, we consider a desired trajectory according to equation (38) to inverse dynamic and the required forces for wheels are obtained as feedforward signal. The same forces are injected to forward dynamic as input and the trajectory will be obtained. By comparing trajectory in forward and inverse dynamic, we check on verification of kinetic modeling.

$$\begin{aligned} V &= t^{1.2} + 1 \\ \beta &= \frac{6\pi}{180} - \frac{6\pi/180}{15} t \\ \dot{\psi} &= 0.15 - \frac{0.15}{15} t \end{aligned} \tag{38}$$

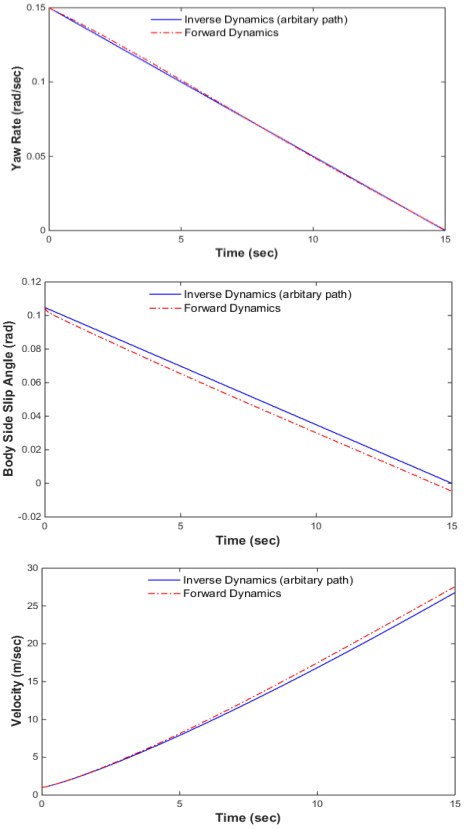

Figure 5. Comparison of the trajectory of state variables in forward and inverse dynamics

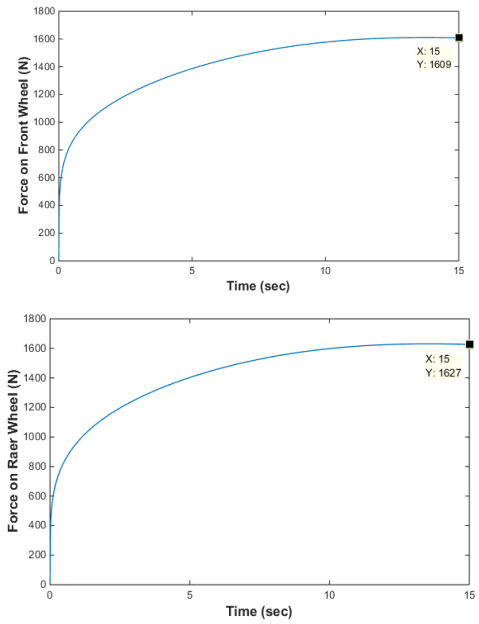

Figure 6. Force on wheels in kinetic simulation

In fact, with considering three desired trajectories for three state variables by inverse dynamic, we can obtain values for control input and after that by using the same values as forward dynamic inputs, we can obtain values for state variables. Using charts according to time, we can make a comparison between primary desired trajectory and the final obtained chart. According to comparison of state variables in forward and inverse kinetics based on figure 5. Wheel forces fit with this work space is according figure 6.

Similar to kinematics results, between trajectory of vehicle in forward and inverse dynamic, there is an acceptable overlap and there is a minimal error more pertinent to numerical solve of non-linear kinetic equation using the software (MATLAB). Also, we can understand the relation between non-linear coupling equation pertinent to state variable and the amount of error. As an example, in light of velocity results which have the maximum error, there is more non-linearity equation and as a result the obtained verification of kinetic model is more precise.

4.3. Simulation related to comparison of two wheel steering and four wheel steering in LQR method

For designing optimal controller, we obtained multipliers matrices which have been linearized surround work space. For two wheel steering and four wheel steering vehicle, values of multiplier matrices are defined in equations (39) and (40), respectively.

$$A=\begin{bmatrix}-0.0011 & 17.1596 & 0.1786\\ -0.0140 & -2.1459 & -0.9731\\ 0.0103 & 13.8337 & -1.7098\end{bmatrix}$$
$$B=\begin{bmatrix}5.9095\times10^{-4} & 6.2348\times10^{-4} & -11.6640 & -5.4955\\ 8.1392\times10^{-6} & 1.7439\times10^{-6} & 0.6326 & 1.5134\\ 2.1131\times10^{-4} & -7.9274\times10^{-5} & 11.6066 & -27.0642\end{bmatrix} \quad (39)$$

$$A=\begin{bmatrix}-0.0026 & 3.9972 & 0.4400\\ -0.0034 & -2.1337 & -0.9732\\ 0.0104 & 14.2498 & -1.7264\end{bmatrix}$$
$$B=\begin{bmatrix}5.9095\times10^{-4} & 6.2158\times10^{-4} & -11.6640 & 7.6669\\ 8.1392\times10^{-6} & -2.6132\times10^{-6} & 0.6326 & 1.5012\\ 2.1131\times10^{-4} & 0 & 11.6066 & -27.8478\end{bmatrix} \quad (40)$$

Using multiplier matrices and weight matrices, after solving Riccati equation mentioned in control theory section, we can obtain matrix S and then optimal gain control matrix for each of the models which are shown in equations (41) and (42) for 2WS and 4WS.

$$S=\begin{bmatrix}8.1654 & -0.7643 & 0.9208\\ -0.7643 & 0.1504 & -0.1034\\ 0.9208 & -0.1034 & 1.2449\end{bmatrix} \Rightarrow K_{Optimal,4WS}=\begin{bmatrix}13.4816 & 83.5000 & 13.9347\\ 15.8783 & 73.6030 & -12.0010\\ -0.0302 & -0.0337 & 0.1127\\ 0.0264 & 0.0765 & -0.2306\end{bmatrix} \quad (41)$$

$$S=\begin{bmatrix}3.9522 & -0.4471 & 0.1826\\ -0.4471 & 0.1646 & -0.1285\\ 0.1826 & -0.1285 & 1.3080\end{bmatrix} \Rightarrow K_{Optimal,2WS}=\begin{bmatrix}23.6801 & 85.8513 & 21.2814\\ 22.6190 & 62.1309 & 2.9448\\ -0.0305 & 0.0305 & 0.0960\\ 0.0297 & 0.0027 & -0.2168\end{bmatrix} \quad (42)$$

Use of each of these optimal gain control matrices in equation (31), finally lead to a series of desired optimal control inputs for each method, these inputs are compared in figure 7.

It can be seen that control inputs for 4WS are more optimized. It means that with less energy consumption in comparison to the more common 2WS model, it provides better response for state variable trajectory according to figure 8. It is obvious that by the aid of 4WS steering system, we can obtain the desired position in a more quick and less oscillated manner. For example, in the velocity curve, 4WS approach to desired value 2.93 second quicker with the precision of one decimal fraction. It suggests 16.86 % improvement in a 15 second time period. While, required force for displacement is optimized. This is due to the increase in the number of control inputs in comparison to freedom degrees and constraint of system which allows for the selection of more optimal options for path planning. Also calculation of cost function in equation (33) for two models showed that 4WS has a cost equal to 157.4 and 2WS has a cost equal to 237.2. This suggests that 4WS is more optimal quantitatively.

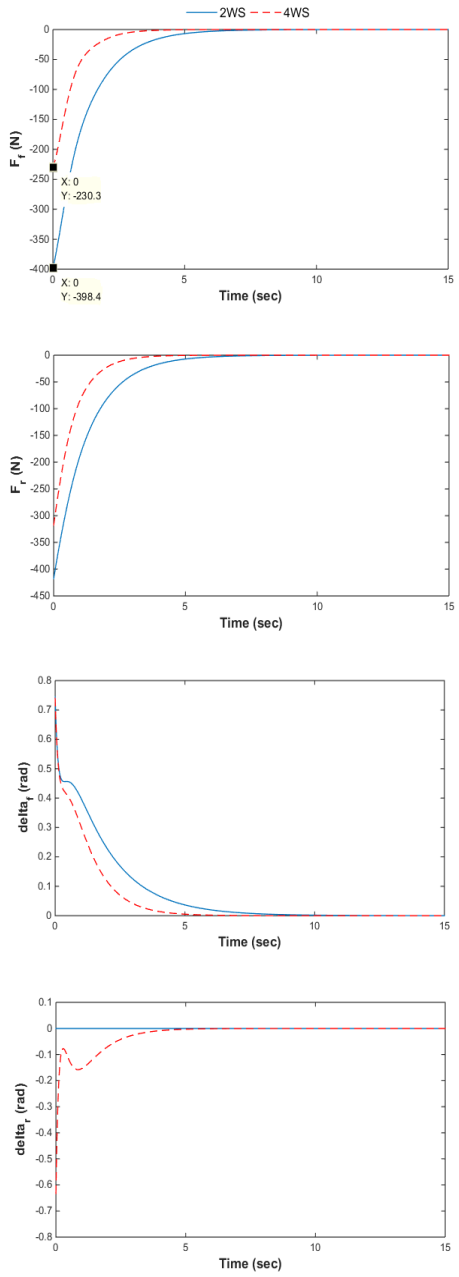

Figure 7. Comparison of the optimal control inputs in both 4WS and 2WS models

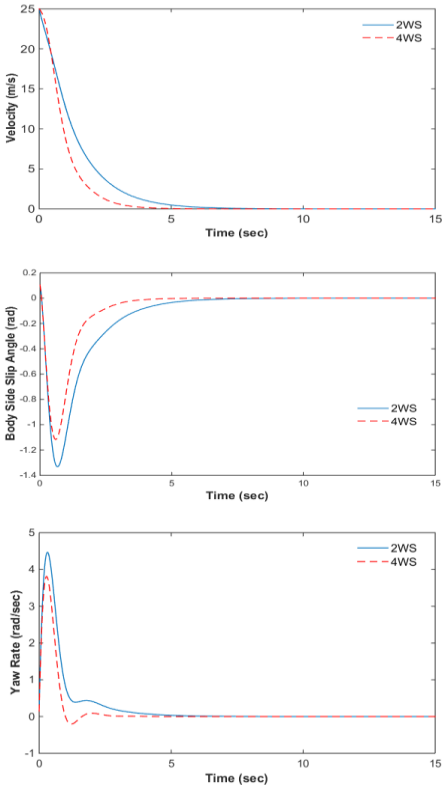

Figure 8. Comparison of the path of state variables in both 4WS and 2WS models

4.4. Simulation for comparison of optimal LQR method and non-optimal method using manual gain matrix for 4WS model

In the previous section, we addressed simulation of optimal LQR method using gain control matrix. In the present section, simulation of optimal LQR method compared to non-optimal method using gain multiplier matrices which have been regulated manually. In equation (43), values of gain multiplier matrices which have been used in simulation software, are presented.

$$K_{Manual} = \begin{bmatrix} 15 & 40 & -100 \\ 20 & 30 & -100 \\ -0.03 & -0.00006 & 0.0008 \\ 0.06 & -0.00005 & 0.0007 \end{bmatrix} \quad (43)$$

Comparison of desired optimal control inputs using LQR method and non-optimal method using gain multiplier matrices are shown in figure 9.

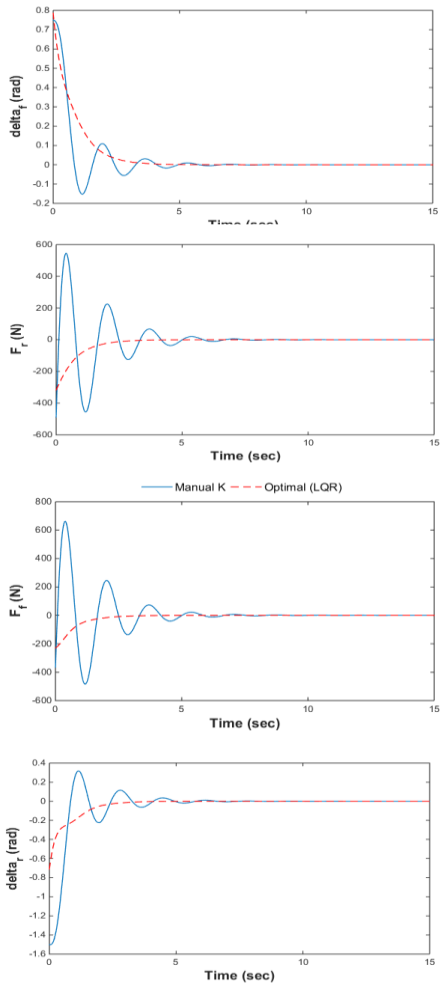

Figure 9. Comparison of the control inputs in both optimal and non-optimal methods

It can be seen that the oscillations of inputs and its increase in the non-linear method comparing to the optimal method is significant. State variables trajectory according to the obtained inputs in the two methods are shown in figure 10. It can be seen that we can obtain a desired position in quicker and less oscillated manner using LQR method in such a way that there is a significant improvement percent for optimal state variables trajectory. For example, for vehicle body yaw rate, the regulation process is accomplished 6.67 seconds sooner using the proposed method of this paper. In simulated time history, there is an improvement equal to 44.47% for the yaw rate regulation of the vehicle movement. In the same manner, improvement in optimal performance in comparison to non-optimal control for side-slip angle and velocity are 23.47% and 13.47%, respectively. While the required force for this displacement has been more optimized. This is due to optimization of this method and obtaining optimal trajectory for vehicle motion between the two positions.

It is worth mentioning that calculation of the cost function for non-optimal state represent higher cost in comparison to optimal state and its value is 710.04%, which in comparison to optimal state (157.37%) is higher. For better comparison of calculated value for cost function in different methods mention in this article, table 2 shows all pertinent results.

Table 2. Resultant Value For The Cost Function For Mentioned Control Algorithms

Cost function value	Modeling	Control method
157.3716	4WS	Optimal
237.1844	2WS	
710.0398	Manual gain matrix	Non-Optimal

As expected, not only optimization resulted in significant reduction of cost function, but also addition of steering control input led to an increase in this improvement, which is mentioned in each section.

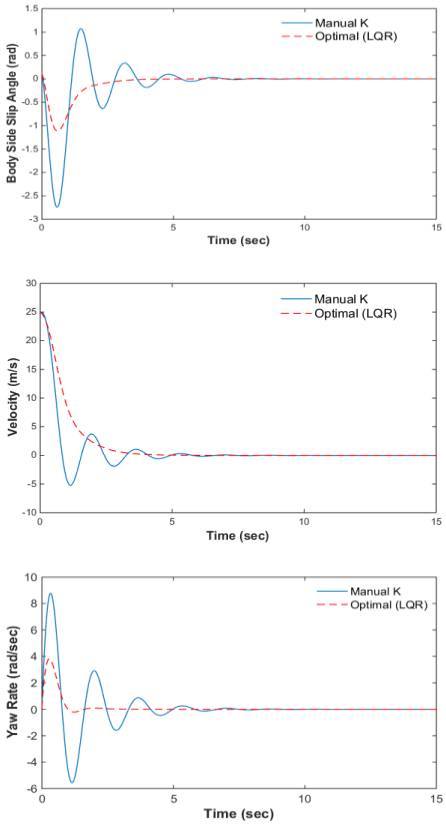

Figure 10. Comparison of the path of state variables in both optimal and non-optimal methods

As mentioned LQR is a closed loop regulator and thus it is robust to some extent against the external disturbances and parametric uncertainties. In order to check the mentioned robustness a regulation is performed in presence the disturbance and uncertainty. Consider that the vehicle is supposed to travel between the following boundaries:

$$\begin{cases} V(0)=0 \\ \beta(0)=0; \\ \psi(0)=0 \end{cases} \begin{cases} V(t_f)=35 \\ \beta(t_f)=\dfrac{6\pi}{180} \\ \psi(t_f)=0.18 \end{cases} \quad (44)$$

The mass of the vehicle is considered about M=1650 kg for designing the controller which is 50 kg less than the actual mass of the modeled vehicle in the plant. Also the following disturbance is implemented on the vehicle dynamics from the road:

$$\underline{u}_{dis} = [-1000sin(t)e^{(-0.5t)}; 1000sin(t)e^{(-0.5t)}; \\ F_3 = -sin(t)e^{(-t)}; F_4 = sin(t)e^{(-t)}] \quad (45)$$

Considering the same controlling gains of equation (43), the actual path of the vehicle in comparison to its desired setpoint can be seen as follow:

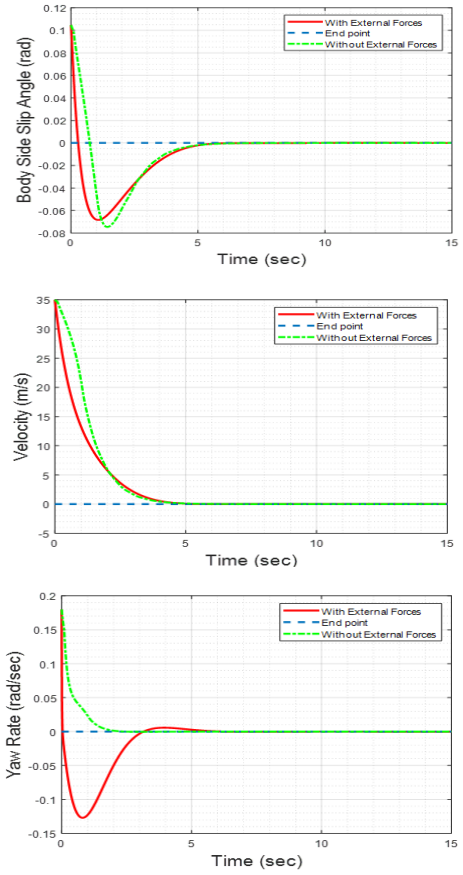

Figure 11. Comparison of the path of state variables in simple situation and in presence of uncertainties

It can be seen that the overall generated path is similar to a simple regulation and despite the negligible oscillations occurred during the implementation of the disturbance, the controller has successfully guided the vehicle to its destination point. The error of the states respect to the setpoint can be seen in the figure 12:

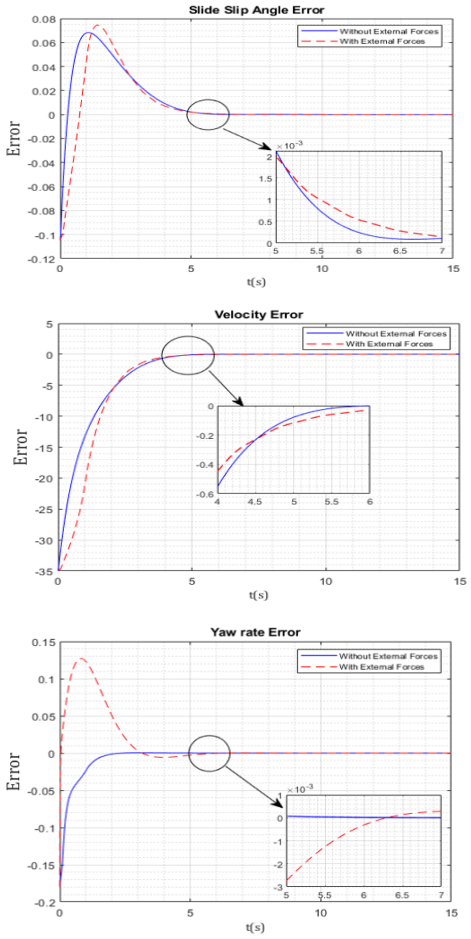

Figure 12. Comparison of the error of state variables in simple situation and in presence of uncertainties

As can be seen at the initial stage of movement, some oscillatory behaviour can be observed since the disturbance domain is maximum during these moments. However the vibration is damped afterwards as a result of feedback based nature of the designed optimal controller and the error converges to zero. This is contributed to the fact that LQR is a Lyapunov based stable controlling strategy. Required controlling effort of the system is also shown as figure 13. Again here the overall trend of required generalized force of the system is the same as LQR regulation. It can be seen that as expected during the moments in which the effect of disturbance is supposed to be compensated, the required force changes according to the error feedback around its mean value in order to neutralize the effect of disturbance and uncertainty. This shows that the

proposed optimal controller not only optimizes the desired objective function, but also is robust against the disturbances and uncertainties as a result of its closed loop nature.

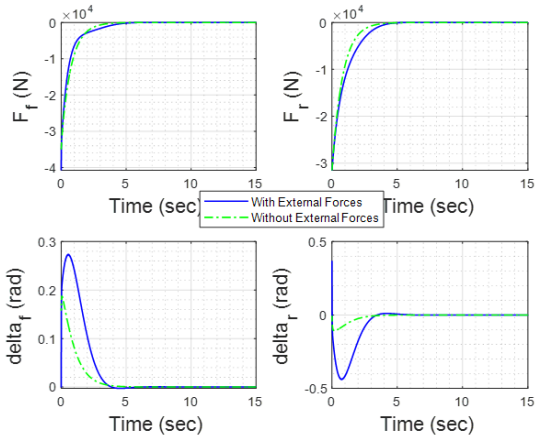

Figure 13. Comparison of the controlling effort between the simple situation and in presence of uncertainties

5. Conclusions

In this paper the complete modeling of a 4 wheel steering vehicle including its dynamics and kinematics based on Jacobian matrix was extracted and using an optimal controller of LQR its optimization process was performed through which the optimal controlling signal and its corresponding optimal path was extracted. It was seen that using the proposed Jacobian based kinematics of the system, dynamics and control of the vehicle can be performed more efficiently. Dynamics of the system was also extracted using Newton-Euler method while the dynamics and sliding of the tire were also considered. Simple and fast closed loop optimization method of LQR was employed to control the vehicle in an optimal and online way between two definite boundaries. Verification of the proposed modelling and controlling was done by conducting some analytic and comparative simulation scenarios in MATLAB. It was seen that between 13%-45% improvement in state accuracy was realized for regulation process of the vehicle while LQR is implemented as its controlling method while the required controlling effort is roughly the same. Also it was proved in this research that by increasing the number of steerable wheels and using the proposed Jacobian based kinematics the possibility of efficient optimization increases since the number of controlling inputs increases and the number of the states is the same. The comparison between these two models shows that the 4wheel steerable system can be optimized with about 16%-23% improvement in the regulation accuracy of the states. It was also shown that the proposed model using the proposed optimal controller can successfully decreases the cost value of the objective function from by about 50.7% rather than the 2 wheel steering system. This improvement is about 351.2% in comparison between the optimal control and simple control of 4 wheel steering system which shows that the proposed model with the proposed optimal controller results in the best performance. Finally it was proved that the proposed optimal controller is robust against the external disturbances and parametric uncertainties since the nature of regulator is closed loop. The controller compensated the implemented disturbances by the aid of its feedback signals and improving its controlling effort which resulted in stability and zero error at the final regulation process.

References:

[1] Spentzas, K., I. Alkhazali, and M. Demic, Kinematics of four-wheel-steering vehicles. Forschung im Ingenieurwesen, 2001. 66(5): p. 211-216.

[2] Spentzas, K., I. Alkhazali, and M. Demic, Dynamics of four-wheel-steering vehicles. Forschung im Ingenieurwesen, 2001. 66(6): p. 260-266.

[3] Singh, A., et al. Study of 4 wheel steering systems to reduce turning radius and increase stability. in International Conference of Advance Research and Innovation (ICARI-2014). 2014.

[4] Wang, D. and F. Qi. Trajectory planning for a four-wheel-steering vehicle. in Robotics and Automation, 2001. Proceedings 2001 ICRA. IEEE International Conference on. 2001. IEEE.

[5] Itoh, H. and A. Oida, Dynamic analysis of turning performance of 4wd-4ws tractor on paved road. Journal of Terramechanics, 1990. 27(2): p. 125-143.

[6] Zhao, Y. and S.L. Bement. Kinematics, dynamics and control of wheeled mobile robots. in Robotics and Automation, 1992. Proceedings., 1992 IEEE International Conference on. 1992. IEEE.

[7] Haiyan, H. and H. Qiang. Three dimensional modeling and dynamic analysis of four-wheel-steering vehicles. Acta Mechanica Sinica, 2003. 19(1): p. 79-88.

[8] Taheri, S., An Alternate Control Algorithm for the Four-Wheel-Steering Vehicles. Vehicle System Dynamics, 1994. 23(S1): p. 497-507.

[9] Korayem, M.H., M. Nazemizadeh, and H.R. Nohooji, Smooth jerk-bounded optimal path planning of tricycle wheeled mobile manipulators in the presence of environmental obstacles. International Journal of Advanced Robotic Systems, 2012. 9(4): p. 105.

[10] Wang, R., et al., Robust lateral motion control of four-wheel independently actuated electric vehicles with tire force saturation consideration. Journal of the Franklin Institute, 2015. 352(2): p. 645-668.

[11] Higuchi, A. and Y. Saitoh, Optimal control of four wheel steering vehicle. Vehicle System Dynamics, 1993. 22(5-6): p. 397-410.

[12] Siahkalroudi, V.N. and M. Naraghi, A Comparison between Zero Steady State Compensators and Optimal Control Regulators in a 4WS vehicle. 2002, SAE Technical Paper.

[13] Mostavi, M., M. Shariatpanahi, and R. Kazemi. A novel optimal four wheel steering control. in Industrial Technology, 2004. IEEE ICIT'04. 2004 IEEE International Conference on. 2004. IEEE.

[14] Wang, Y. and M. Nagai. Integrated control of four-wheel-steer and yaw moment to improve dynamic stability margin. in Decision and Control, 1996., Proceedings of the 35th IEEE Conference on. 1996. IEEE.

[15] Hongming, L. and L. Shaona, Closed-loop handling stability of 4WS vehicle with yaw rate control/Bocna vodljivost zaprtozancnega sistema voznika in vozila s sistemom 4WS s krmiljenjem hitrosti vrtenja okrog navpicne osi. Strojniski Vestnik-Journal of Mechanical Engineering, 2013. 59(10): p. 595-605.

[16] Akita, T. and K. Satoh, Development of 4WS control algorithms for an SUV. JSAE review, 2003. 24(4): p. 441-448.

[17] Lee, A., Design of stability augmentation systems for automotive vehicles. Journal of Dynamic Systems, Measurement, and Control, 1990. 112(3): p. 489-495.

[18] Matsumoto, N. and M. Tomizuka, Vehicle lateral velocity and yaw rate control with two independent control inputs. Journal of Dynamic systems, measurement, and Control, 1992. 114(4): p. 606-613.

[19] Mostavi, M., R. Kazemi, and M. Shariatpanahi. An optimal control of four wheel steering vehicles. in to appear in WSEAS Conf.: Citeseer.

[20] Anderson, B.D., J. Pren, and S. Dickerson, Linear optimal control. 1971, American Society of Mechanical Engineers.

[21] Ogata, K. and Y. Yang, Modern control engineering. Vol. 4. 2002: Prentice hall India.

6. Biography

H. Tourajizadeh was born in Tehran, Iran on October 30, 1984. He has received his Ph.D. from IUST in the field mechanics, branch of control and robotics. More than 35 journal papers, 15 conference papers, 1 published book, 1-chapter book and 2 booked inventions are the results of his researches so far. He has been involved in teaching and research activities for more than 10 years in different universities and he is now assistant professor of Kharazmi University from 2013. His research interests include robotics, automotive engineering, control and optimization.

M. Sarvari was born in Moghan, Ardebil, Iran on September 5 , 1991. He has received his MSc. From KHU Tehran in the field mechanics, branch of control and robotics.

S. Ordoo was born in Dezful, Khuzestan, Iran on Aguest 23, 1989. He has received his MSc. From KHU of Tehran in the field mechanics, branch of control and robotics.